

High Sensitivity Tests of Quantum Gravity induced Spin Statistics Deformation

K. Piscicchia

Centro Ricerche Enrico Fermi
LNF (INFN)

on behalf of the VIP-2 collaboration

The Hitchhiker's Advanced Guide to Quantum Collapse Models ...

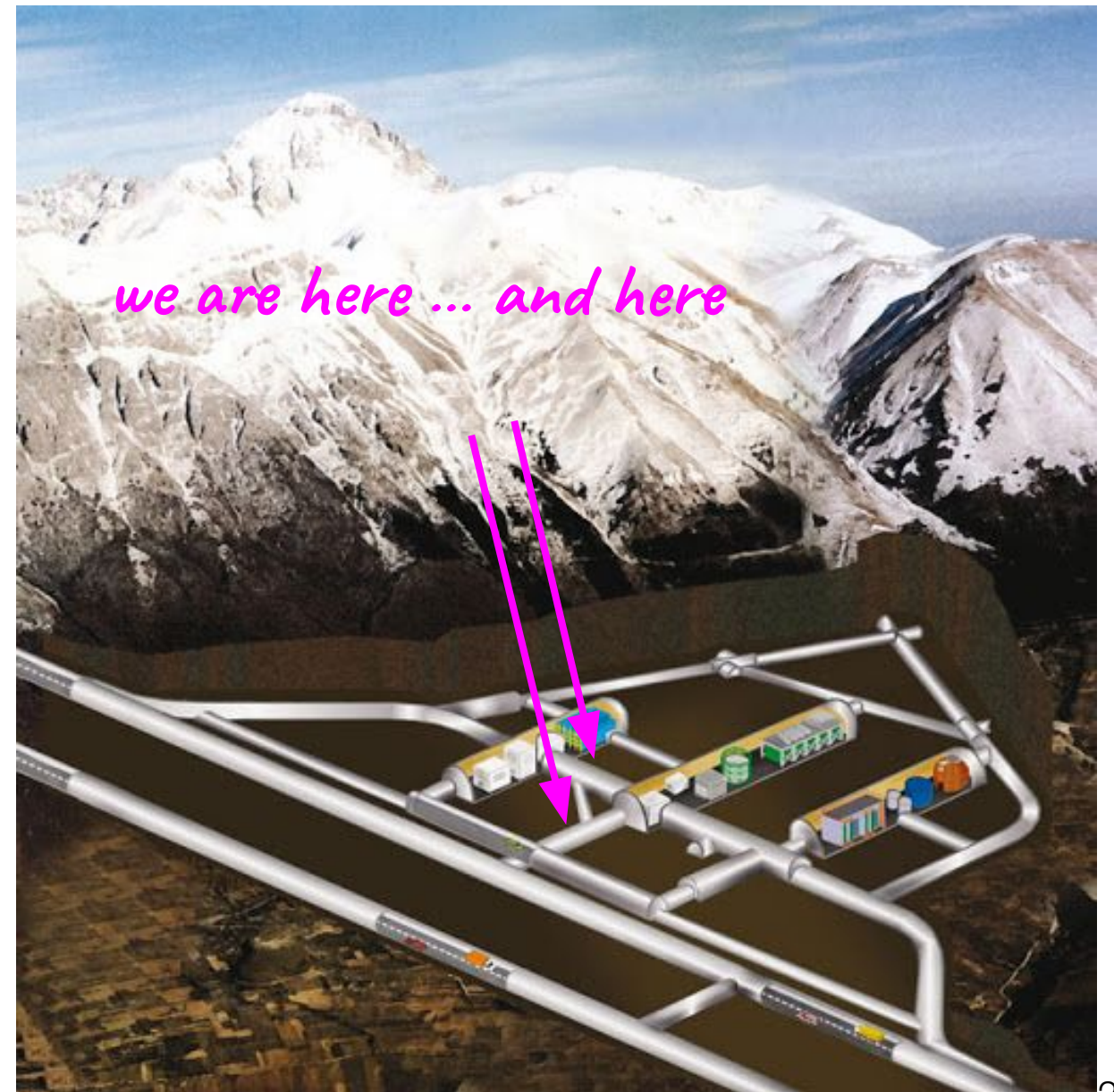
31 Oct - 4 Nov 2022, LNF (INFN), Italy

We acknowledge the John Templeton Foundation for the project QUBO
(Exploring the QUantum Boundaries of many-body systems – an Odyssey into
the gravity related collapse models), Grant 62099

The LNGS laboratories environment

The experiments are performed in the low-background environment of the underground *Gran Sasso National Laboratory of INFN*:

- overburden corresponding to a minimum thickness of 3100 m w.e.
- the muon flux is reduced by almost six orders of magnitude, to a flux of three oom.
- the main background source consists of γ -radiation produced by long-lived γ -emitting primordial isotopes and their decay products.



Spin statistics theorem (Fierz 1939, Pauli 1940, Schwinger, Lüders, Zumino...)

Postulates: inhomogeneous Lorentz group, locality, microcausality, vacuum is the state of lowest energy, Hilbert space metric positive definite, vacuum is not identically annihilated by a field \rightarrow

(pseudo)scalar fields commute and spinor fields anticommute

Models of PEP violation:

- Pioneering work of Fermi, Gentile, Green ...
- Ignatiev and Kuzmin [A.Y. Ignatiev, V.A. Kuzmin, Proceedings of the Seminar, Tbilisi, USSR, 15-17 April 1986] (deformation of the standard Fermi oscillator)

$$\begin{array}{ll} a^+|0\rangle = |1\rangle & a|0\rangle = 0 \\ a^+|1\rangle = \beta|2\rangle & a|1\rangle = |0\rangle \\ a^+|2\rangle = 0 & a|2\rangle = \beta|1\rangle \end{array}$$

- **Rahal and Campa** [V. Rahal, A. Campa, Thermodynamical implications of a violation of the Pauli principle. Phys. Rev. A 38(7), 3728–3731 (1988)] **global w.f. of the electrons is not exactly antisymmetric, PEP holds as long as the number of wrongly entangled pairs is small.**

O. W. Greenberg (AIP Conf. Proc. 545): 113-127, 2004 “Possible external motivations for violation of statistics include: (a) violation of CPT, (b) violation of locality, (c) violation of Lorentz invariance, (d) extra space dimensions, (e) discrete space end or time and (f) non commutative spacetime”



Two classes of PEP violation models:

Static deformation of comm/anticomm relations - Greenberg & Mohapatra, quon model [O.W. Greenberg, R.N. Mohapatra, Phys. Rev. Lett. 59(22), 2507–2510 (1987)]

$$a_k a_l^\dagger - q a_l^\dagger a_k = \delta_{k,l}$$

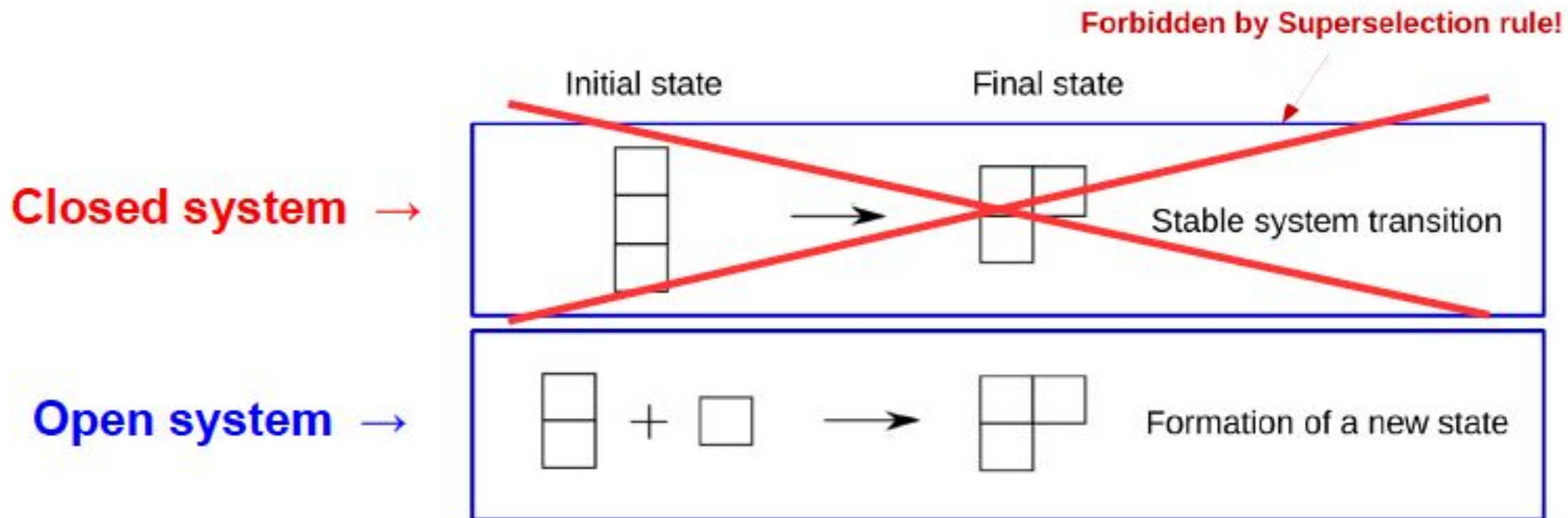
is subject to the **M-G Superselection Rule** -> can be only tested with **open systems**.

Space-time properties - Balachandran, Addazi, Marcianò, Mavromatos ...
unrestricted by **M-G Superselection Rule** -> can be tested with **closed systems**.
DAMA/LIBRA, BOREXINO ...

VIP-2 tests the Pauli Exclusion Principle (PEP) (spin-statistics) for electrons in a clean environment (LNGS) using a method which respects the

Messiah-Greenberg superselection rule :

Superpositions of states with different symmetry are not allowed → transition probability between two symmetry states is **ZERO**



VIP sets the best limit on PEP violation for an elementary particle respecting the M-G superselection rule

A high-altitude mountain landscape with a bright sun in a clear blue sky. The foreground shows rugged, rocky terrain with patches of snow. The background features a vast range of mountains under a clear sky. The sun is positioned in the upper right quadrant, creating a lens flare effect.

VIP-2 Closed Systems

PEP violation in quantum gravity

Quantum gravity models can embed PEP violating transitions

PEP is a consequence of the spin statistics theorem based on: Lorentz/Poincaré and CPT symmetries; locality; unitarity and causality. Deeply related to the very same nature of space and time



non-commutativity of space-time operators is common to several quantum gravity frameworks (e.g. k -Poincaré, θ -Poincaré)



non-commutativity induces a deformation of the Lorentz symmetry and of the locality → naturally encodes the violation of PEP not constrained by MG

PEP violation is suppressed with $\delta^2 (E, \Lambda)$

E is the characteristic transition energy, Λ is the scale of the space-time non-commutativity emergence.

A. P. Balachandran, G. Mangano, A. Pinzul and S. Vaidya, *Int. J. Mod. Phys. A* 21 (2006) 3111

A.P. Balachandran, T.R. Govindarajan, G. Mangano, A. Pinzul, B.A. Qureshi and S. Vaidya, *Phys. Rev. D* 75 (2007)

A. Addazi, A. Marciano, *Int.J.Mod.Phys.A* 35 (2020) 32, 2042003

testing PEP violation in quantum gravity

Theoretical prediction *Int.J.Mod.Phys.A* 35 (2020) 32, 2042003

specific calculation of atomic levels transitions probabilities for θ -Poincaré

$$W \simeq W_0 \phi_{PEPV}, \quad \phi_{PEPV} = \delta^2 \simeq \frac{D E_N \Delta E}{2 \Lambda \Lambda} \quad \phi_{PEPV} = \delta^2 \simeq \frac{C \bar{E}_1 \bar{E}_2}{2 \Lambda \Lambda}$$

for non-vanishing (vanishing) electric like components of the $\theta_{\mu\nu}$ tensor.

Connection with quon algebra (in the case of quon fields however the q factor does not show any energy dependence):

$$q(E) = -1 + 2\delta^2(E)$$

An experimental bound on the probability that PEP may be violated in atomic transition processes, straightforwardly translates into a bound on the new physics scale Λ , consistently with the choice of the θ_{0i} components.

Experimental Setup

High purity Ge detector measurement:

- high purity co-axial p-type germanium detector (HPGe), diameter of 8.0 cm, length of 8.0 cm, surrounded by an inactive layer of lithium-doped germanium of 0.075 mm.
- Target material: three cylindrical sections of radio-pure Roman lead (5 cm thick) completely surrounding the detector -> **High energy transitions**

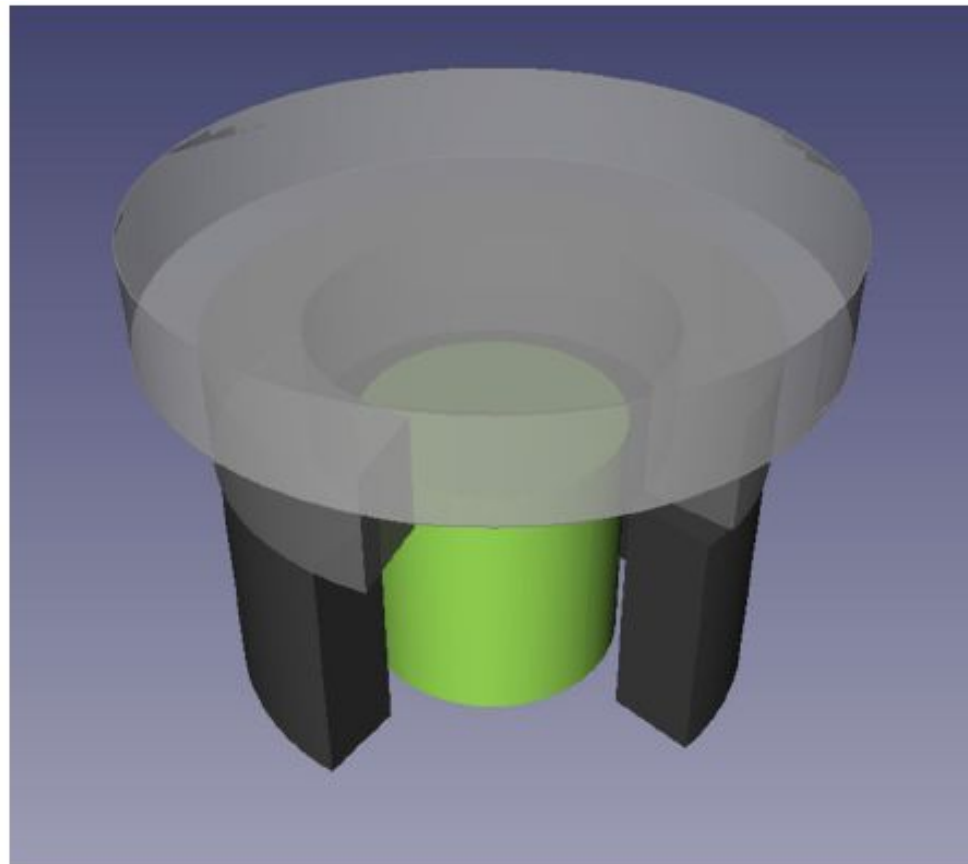


Fig. 1 Schematic representation of the Ge crystal (in green) and the surrounding lead target cylindrical sections (in grey)

Experimental Setup

- **Passive shielding:**
outer part lead (30 cm from the bottom and 25 cm from the sides). Inner layer (5 cm) electrolytic copper.
On the bottom and on the sides 5 cm thick 10B-polyethylene plates reduce the neutron flux towards the detector.
- **shield + cryostat enclosed in air tight steel housing flushed with nitrogen to avoid contact with external air (thus radon).**

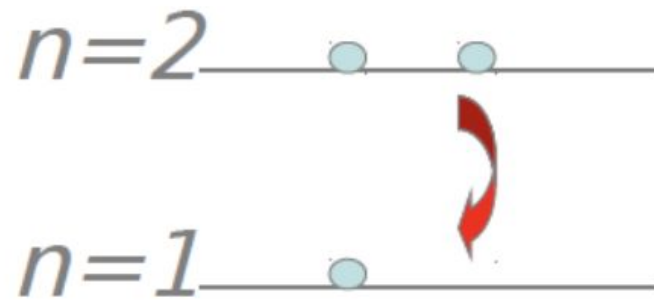


- Whole detector is characterised and all of its components have been put into a validated Monte Carlo (MC) code based on GEANT4.
- Acquisition time $\Delta t \approx 70d \approx 6.1 \cdot 10^6s$

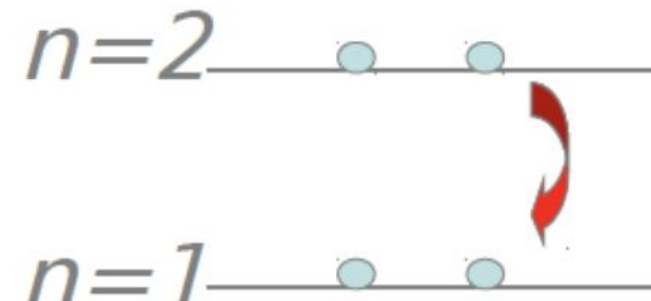
K. P. et al., Eur. Phys. J. C (2020) 80: 508
<https://doi.org/10.1140/epjc/s10052-020-8040-5>

Strategy of the measurement

- Aim of the measurement: search for the X-rays signature of PEP-violating K_{α} and K_{β} transitions in Pb, when the 1s level is already occupied by two electrons.
- Transitions are shifted with respect to the standard ones due to additional shielding.



Normal 2p \rightarrow 1s transition



2p \rightarrow 1s transition violating Pauli principle

- Deformation of the algebra preserves, at the first order, standard atomic transition probabilities, the violating transition probabilities being dumped by factors $\delta^2(E)$ \rightarrow transitions to the 1s level from levels higher than 4p can be neglected.

- PEP violating K lines energies based on multi configuration Dirac-Fock and General Matrix Elements numerical code.

Transitions in Pb	allow. (keV)	forb. (keV)
1s - 2p _{3/2} K _{α1}	74.961	73.713
1s - 2p _{1/2} K _{α2}	72.798	71.652
1s - 3p _{3/2} K _{β1}	84.939	83.856
1s - 4p _{1/2(3/2)} K _{β2}	87.320	86.418
1s - 3p _{1/2} K _{β3}	84.450	83.385

Strategy of the measurement

- The *pdf* of the expected number of total signal counts S given the measured distribution is:

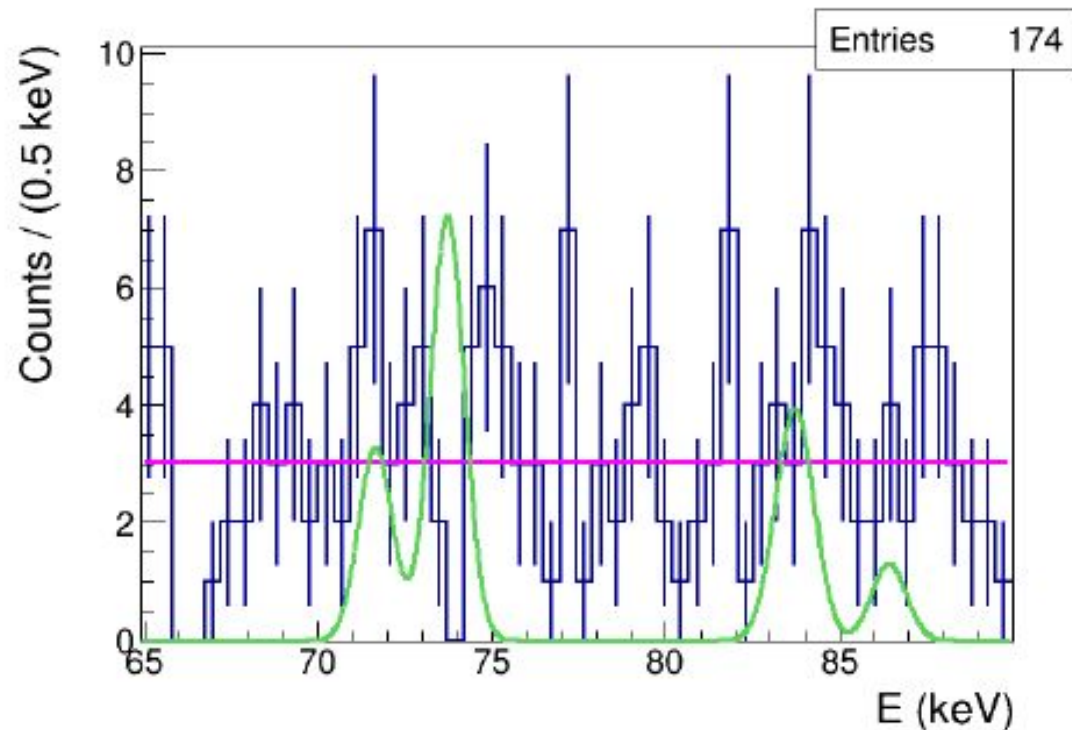


FIG. 1. The measured X-ray spectrum, in the region of the K_α and K_β standard and violating transitions in Pb, is shown in blue; the magenta line represents the fit of the background distribution. The green line corresponds to the shape of the expected signal distribution (with arbitrary normalization) for $\theta_{0i} \neq 0$.

The prior for S consistent with existing limits [Found. Phys. 42, 1015-1030 (2012)].



$$P(S|data) = \int_0^\infty \int_{\mathcal{D}_p} P(S, B|data, \mathbf{p}) d^m \mathbf{p} dB$$

$$P(S, B|data, \mathbf{p}) =$$

$$= \frac{P(data|S, B, \mathbf{p}) \cdot f(\mathbf{p}) \cdot P_0(S) \cdot P_0(B)}{\int P(data|S, B, \mathbf{p}) \cdot f(\mathbf{p}) \cdot P_0(S) \cdot P_0(B) d^m \mathbf{p} dS dB}$$

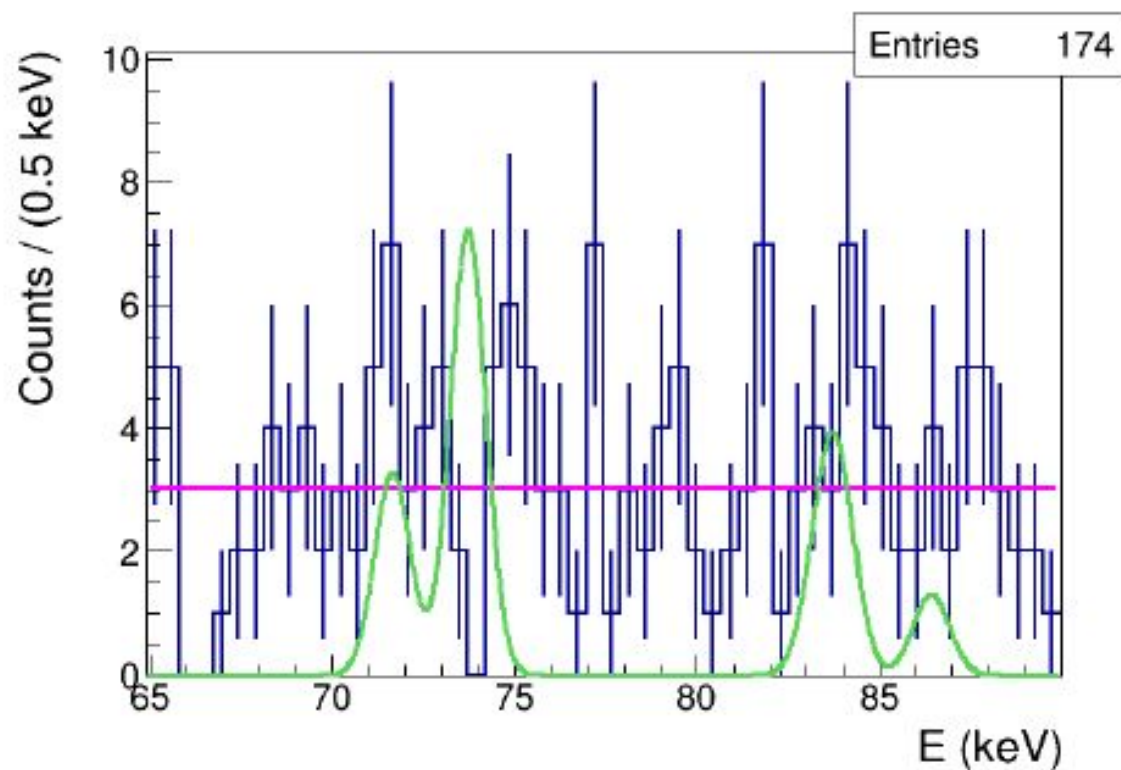
- the likelihood is weighted on the joint *pdf* of the experimental parameters

$$P(data|S, B, \mathbf{p}) = \prod_{i=1}^N \frac{\lambda_i(S, B, \mathbf{p})^{n_i} e^{-\lambda_i(S, B, \mathbf{p})}}{n_i!}$$

$$\lambda_i(S, B, \mathbf{p}) = B \cdot \int_{\Delta E_i} f_B(E, \alpha) dE + S \cdot \int_{\Delta E_i} f_S(E, \sigma) dE$$

Statistical model

- First analysis which accounts for the predicted energy dependence of the PEP violation probability. Expected rate of $K_{\alpha 1}$ transitions:



$$\Gamma_{K_{\alpha 1}} = \frac{\delta^2(E_{K_{\alpha 1}})}{\tau_{K_{\alpha 1}}} \cdot \frac{BR_{K_{\alpha 1}}}{BR_{K_{\alpha 1}} + BR_{K_{\alpha 2}}} \cdot 6 \cdot N_{atom} \cdot \epsilon(E_{K_{\alpha 1}}).$$

- normalized shape of the signal distribution:

$$f_S(E, k) = \frac{1}{N} \cdot \sum_{K=1}^{N_K} \Gamma_K \frac{1}{\sqrt{2\pi\sigma_K^2}} \cdot e^{-\frac{(E-E_K)^2}{2\sigma_K^2}}$$

FIG. 1. The measured X-ray spectrum, in the region of the K_{α} and K_{β} standard and violating transitions in Pb, is shown in blue; the magenta line represents the fit of the background distribution. The green line corresponds to the shape of the expected signal distribution (with arbitrary normalization) for $\theta_{0i} \neq 0$.

- normalization condition:

$$\int_{\Delta E} f_S(E) dE = 1 \Rightarrow N = \sum_{K=1}^{N_K} \Gamma_K.$$

Statistical model

- probability to observe n transitions in the time t :

$$P(n; t) = \frac{(\Gamma_{K\alpha_1} t)^n e^{-\Gamma_{K\alpha_1} t}}{n!}, \quad \mu_{K\alpha_1} = \Gamma_{K\alpha_1} \cdot \Delta t.$$

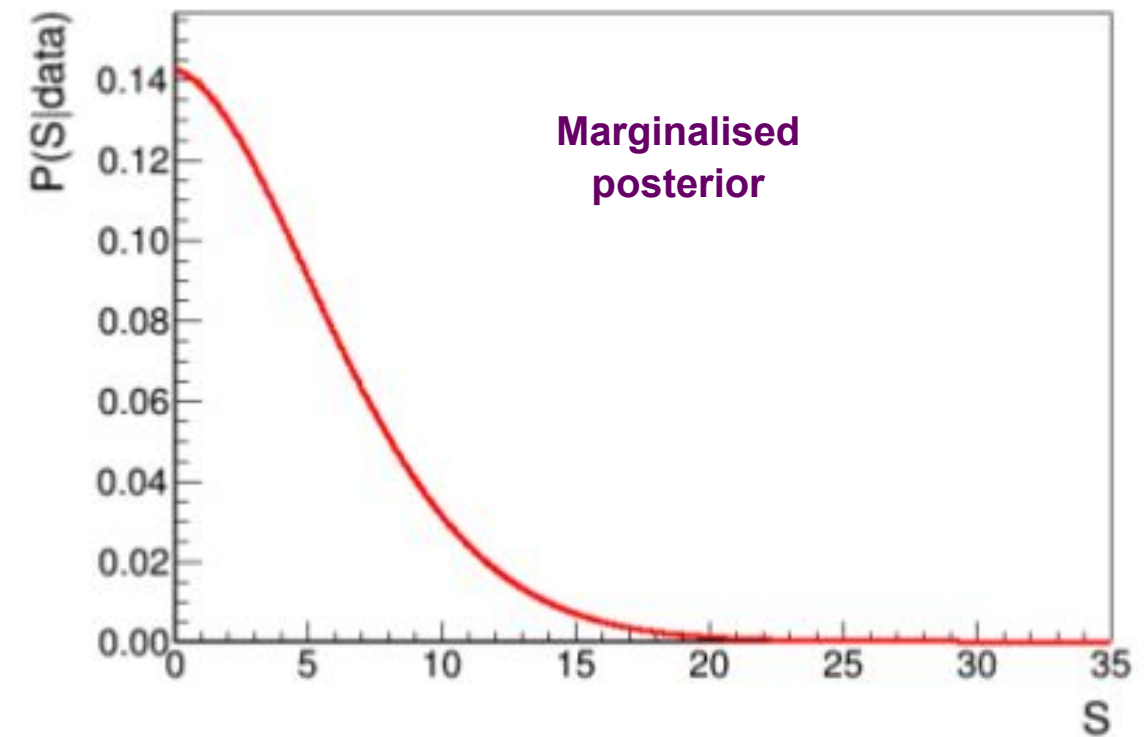
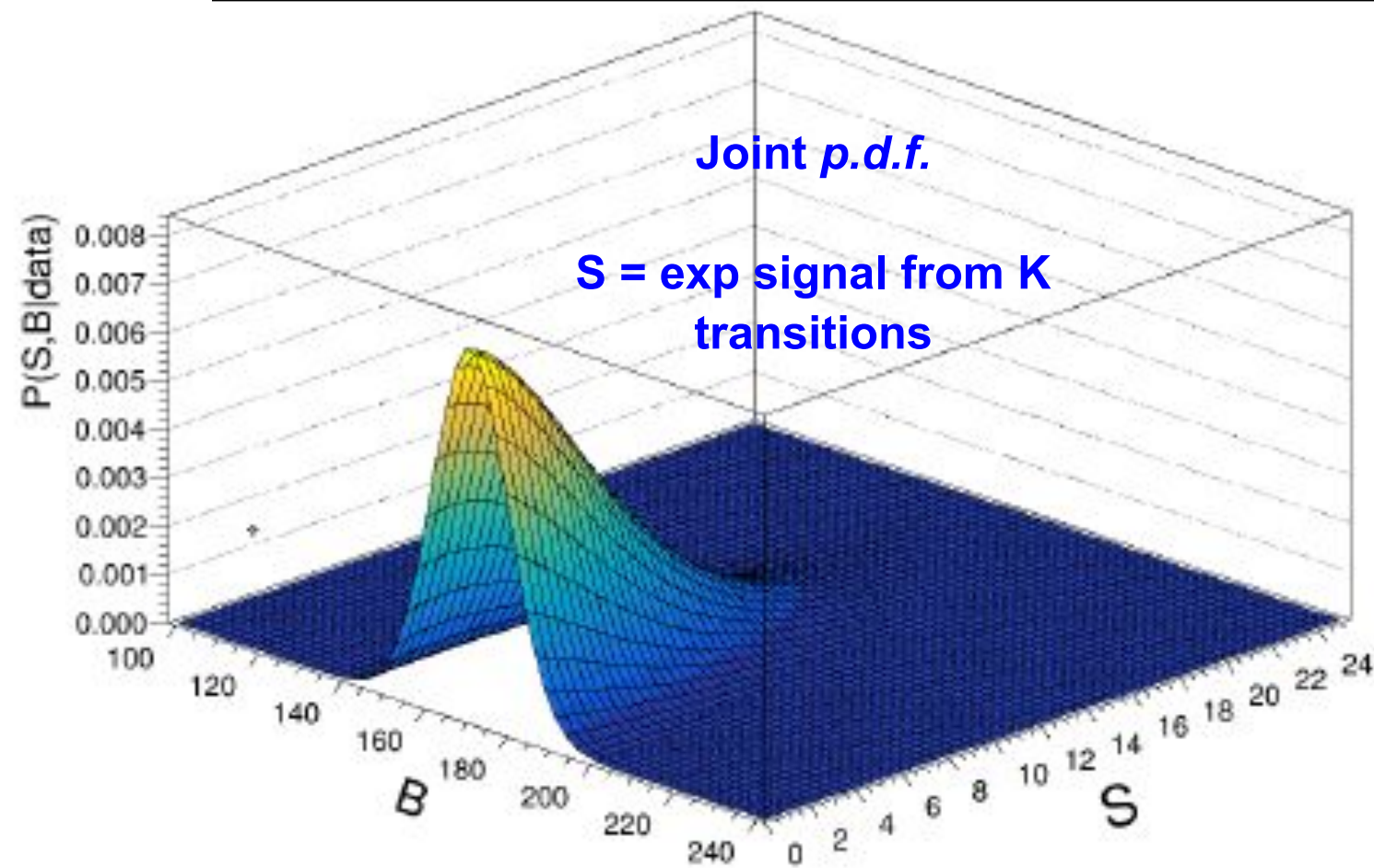
- From which the upper limit on the non-commutativity scale is:

$$\mu = \sum_{K=1}^{N_K} \mu_K = \frac{\aleph}{\Lambda^k} < \bar{S}$$

- with:

$$\tilde{P}(\bar{S}) = \int_0^{\bar{S}} P(S|data) dS = \Pi,$$

Results



From which an upper limit on the non-commutativity scale is obtained (90% Probability):

θ_{0i}	\bar{S}	lower limit on Λ (Planck scales)
$\theta_{0i} = 0$	13.2990	$6.9 \cdot 10^{-2}$
$\theta_{0i} \neq 0$	18.1515	$2.6 \cdot 10^2$

A different parametrization

- For a generic NCQG model deviations from the PEP in the commutation/anti-commutation relations can be parametrized as:

$$a_i a_j^\dagger - q(E) a_j^\dagger a_i = \delta_{ij}$$

- E = energy level difference, i.e. to the PEP violating X-ray line energy. q is related to the PEP violation probability by:

$$q(E) = -1 + 2\delta^2(E)$$

- phenomenological method includes, through an analytic expansion, the infrared limit for several different UV-complete quantum field theories:

$$M_k : \quad \delta^2(E) = \frac{E^k}{\Lambda^k} + O(E^{k+1})$$

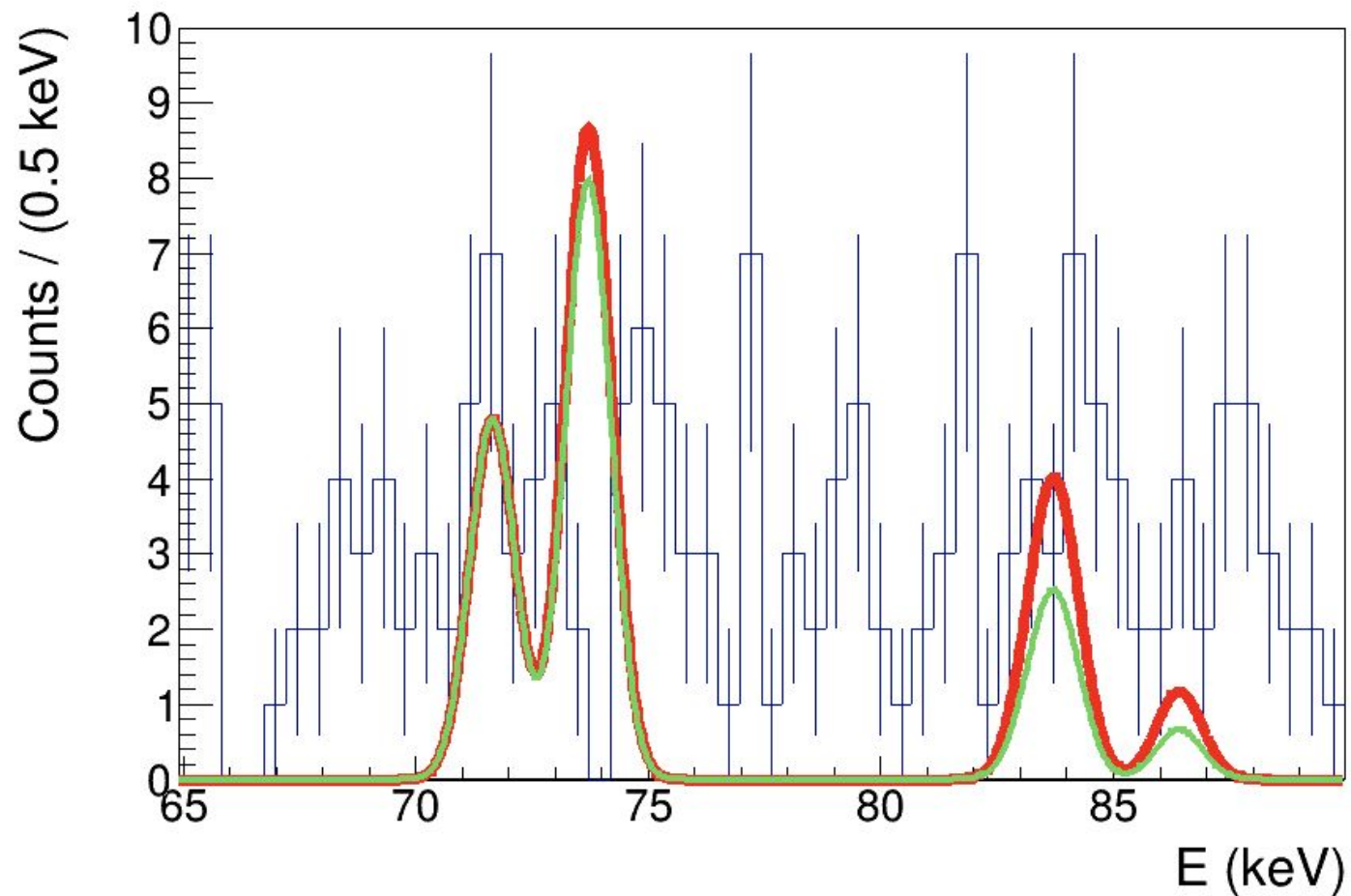
A different parametrization

- constraints on the PEP violation prob. traduce into constraints on Λ specific for each M_k parametrization.
- $k = 1$ corresponds to k -Poincaré. Different quantization procedures lead to different predictions:
 - Arzano-Marcianò procedure - PEP violation is suppressed with a probability proportional to
$$\delta^2 = E / \Lambda$$
 - Freidel-Kowalski-Glikman-Nowak procedure - PEP violation is missing.

So experimental investigation of statistics violations provides important down-top indications on the “right” quantization procedure.

A different parametrization

- The normalised signal shape for the M_3 parametrization is given by:



**Neglecting the PEP violation
prob. energy dependence**

**Considering the PEP violation
prob. energy dependence
for $k = 3$**

- The sensitivity on Λ increases with E \rightarrow the analysis is repeated by searching for PEP violation signal in $K\alpha$, $K\beta$ and $K\alpha + K\beta$ transitions.

Constraint on k -Poincaré

- the highest sensitivity is provided by the survey on the whole K complex which gives:

A_i, M_k	\bar{S}	lower limit on Λ in unit of Planck scale
$A_1, k = 1$	11.4913	$2.1 \cdot 10^{21}$
$A_1, k = 2$	11.3776	$1.4 \cdot 10^{-1}$
$A_1, k = 3$	11.2610	$4.9 \cdot 10^{-9}$
$A_2, k = 1$	15.1408	$2.8 \cdot 10^{21}$
$A_2, k = 2$	15.1640	$1.4 \cdot 10^{-1}$
$A_2, k = 3$	15.1859	$5.1 \cdot 10^{-9}$
$A_3, k = 1$	18.7270	$4.2 \cdot 10^{21}$
$A_3, k = 2$	19.1847	$1.6 \cdot 10^{-1}$
$A_3, k = 3$	19.5993	$5.6 \cdot 10^{-9}$

preliminary,
paper under
finalization

- which constrains the energy scale at which space-time non commutativity would emerge in the AM procedure far above the Planck scale!

Future perspectives

- **Theoretical investigation of signature of physics beyond the Standard Model, possibly related to the Lorentz or CPT symmetries violations, existence of extra-dimensions, non-locality or non-commutativity of space-time structure.**
- **In particular PEP violation may manifest non-isotropy. Angular dependence of the PEPV emission is presently under study.**
- **A dedicated experiment with directionality capabilities, based on beyond the state-of-art, high efficiency over a broad energy range, and high-energy resolution x-ray detector systems is in R&D phase.**



Thank you

Among the experimental uncertainties the only ones which significantly affect ρ are those which characterize the shape of background (parametrized by the vector \vec{b}) and the resolutions (σ) at the energies of the violating transitions (the resolutions are reported in Table II). All the other experimental parameters are affected by relative uncertainties of the order of 1% (or less), which are neglected, hence $\rho = (\dots ; \dots)$.

TABLE II. The table summarizes the resolutions (σ) in keV, at the energies of the PEP violating K_α and K_β transitions.

Transitions in Pb	σ (keV)	error (keV)
$K_{\alpha 1}$	0.492	0.037
$K_{\alpha 2}$	0.491	0.037
$1s - 3p_{3/2} K_{\beta 1}$	0.497	0.036
$1s - 4p_{1/2(3/2)} K_{\beta 2}$	0.498	0.036
$1s - 3p_{1/2} K_{\beta 3}$	0.497	0.036

TABLE III. The table summarizes the values of the branching ratios of the considered atomic transitions and the detection efficiencies at the energies corresponding to the K_α and K_β forbidden transitions.

Forb. transitions	BR	ϵ
$K_{\alpha 1}$	0.462 ± 0.009	$(5.39 \pm 0.11) \cdot 10^{-5}$
$K_{\alpha 2}$	0.277 ± 0.006	$(4.43^{+0.10}_{-0.09}) \cdot 10^{-5}$
$K_{\beta 1}$	0.1070 ± 0.0022	$(11.89 \pm 0.24) \cdot 10^{-5}$
$K_{\beta 2}$	0.0390 ± 0.0008	$(14.05^{+0.29}_{-0.28}) \cdot 10^{-5}$
$K_{\beta 3}$	0.0559 ± 0.0011	$(11.51^{+0.24}_{-0.23}) \cdot 10^{-5}$

B. Normalized background shape

The normalized background shape is obtained from the best maximum log-likelihood fit to the measured spectrum, excluding $3\sigma_K$ intervals centered on the mean energies E_K of each violating transition. The best fit yields a flat background amounting to $L(E) = \alpha = (3.05 \pm 0.29)$ counts/(0.5 keV), the errors contain both statistical and systematic uncertainties. The normalized background shape is then:

$$f_B(E) = \frac{L(E)}{\int_{\Delta E} L(E) dE}. \quad (18)$$

C. Prior distributions

For positive values of B we choose a Gaussian prior distribution, with expected value $B_0 = \langle B \rangle_G = \int_{\Delta E} L(E) dE$ and standard deviation $\sigma_B = \sqrt{B_0}$. Zero probability is assigned to negative values of B . As a check a Poissonian prior was tested for B , in this case from the Bayes theorem the expected value is $\langle B \rangle_P = B_0 + 1$ and $\sigma_B = \sqrt{\langle B \rangle_P}$. The upper limit on \bar{S} is found not to be affected by this choice, within the experimental uncertainty.

For what concerns the choice of the prior $P_0(S)$, considered the a priori ignorance on the value of S , we opt for a uniform distribution in the range $(0 \div S_{max})$, where S_{max} represents the maximum value of PEP violating X-ray counts in Pb, compatible with the best independent experimental bound (Ref. [55]) on the PEP violation probability. S_{max} is then obtained from Eq. 3 in Ref. [55], by substituting the number of free electrons in the conduction band of the target, the mean number of interactions and the efficiency with the corresponding parameters which characterise our experimental apparatus (see Tables III and V). We obtain $S_{max} \approx 1433$ and the prior on S is

$$P_0(S) = \begin{cases} \frac{1}{S_{max}} & 0 \leq S \leq S_{max} \\ 0 & \text{otherwise} \end{cases} . \quad (19)$$

TABLE V. Values of the parameters which characterise the Roman lead target, from left to right: free electron density, volume, mass and number of free electrons in the conduction band.

$n_e(\text{m}^{-3})$	$V(\text{cm}^3)$	$M(\text{g})$	N_{free}
$1.33 \cdot 10^{29}$	$2.17 \cdot 10^3$	22300	$2.89 \cdot 10^{26}$

Quantum Gravity test with HPGe data taking 2016-2017

- The transition energies are calculated with an accuracy of few eV, based on a Dirac-Hartree-Slater calculation that includes the Breit interaction and QED corrections
- efficiency function obtained by MC simulations
- total acquisition time $\Delta t \approx 70d \approx 6.1 \cdot 10^6s$

Transitions in Pb	allow.	forb.
1s - 2p _{3/2} K _{α1}	74.969	73.713
1s - 2p _{1/2} K _{α2}	72.805	71.652
1s - 3p _{3/2} K _{β1}	84.938	83.85644
1s - 4p _{1/2(3/2)} K _{β2}	87.300	86.417790
1s - 3p _{1/2} K _{β3}	84.450	83.38536

Forb. transitions	$\epsilon_{BR,1,2}$	$\epsilon_{x,1,2}$
K _{α1}	0.462 ± 0.009	$(5.39 \pm 0.11) \cdot 10^{-5}$
K _{α2}	0.277 ± 0.006	$(4.43^{+0.10}_{-0.09}) \cdot 10^{-5}$
K _{β1}	0.1070 ± 0.0022	$(11.89 \pm 0.24) \cdot 10^{-5}$
K _{β2}	0.0390 ± 0.0008	$(14.05^{+0.29}_{-0.28}) \cdot 10^{-5}$
K _{β3}	0.0559 ± 0.0011	$(11.51^{+0.24}_{-0.23}) \cdot 10^{-5}$

**Neglecting the PEP violation prob.
energy dependence**

**Considering the PEP violation prob.
energy dependence
for k = 3**

